JOURNAL OF EXPERIMENTAL AND THEORETICAL PHYSICS, 2024, Vol. 166, No. 5(11), pp. 728–734

STATISTICAL, NONLINEAR, AND SOFT MATTER PHYSICS

LOW-THRESHOLD DECAY OF ORDINARY MICROWAVE IN THE PRESENCE OF LARGE-SCALE COHERENT STRUCTURES IN A RAREFIED PLASMA

© 2024 A. Yu. Popov[a,*], E. Z. Gusakov[a], A. A. Nagovitsyn[a], L. V. Simonchik[b], M. S. Usachenok[b]

[a] *Ioffe Institute Russian Academy of Sciences, Saint Petersburg, 194021, Russia*
[b] *Stepanov Institute of Physics, National Academy of Sciences of Belarus, Minsk, 220072, Republic of Belarus*
**e-mail: a.popov@mail.ioffe.ru*

Received April 01, 2024

Revised June 17, 2024

Accepted June 17, 2024

Abstract. The scenario of low-threshold decay of an ordinary microwave with a frequency corresponding to the second harmonic of electron cyclotron resonance, leading to the excitation of two electron Bernstein waves two-dimensionally localized in a large-scale coherent structure in a rarefied plasma, has been investigated. Using the proposed model, estimates for the threshold of this nonlinear phenomenon were obtained for ASDEX-Upgrade and Wendelstein 7-X facilities, as well as in a model experiment on a linear device.

DOI: 10.31857/S004445102411e178

1. INTRODUCTION

Recent research has been actively focused on low-threshold nonlinear phenomena in the interaction of high-power microwaves with plasma in toroidal magnetic confinement devices. Among them is the anomalous scattering of the pump wave with frequency shifts of the scattered signal both downward and upward relative to the generator (gyrotron) frequency, which has been observed in various experimental facilities [1–4]. At first glance, the experimental manifestation of these effects contradicts theoretical results, since according to established views from the 1990s, the thresholds for exciting nonlinear phenomena in inhomogeneous plasma (particularly in various scenarios of parametric decay instability of microwaves) exceed 5 MW [5]. This value, caused by large convective losses of daughter waves from the finite-sized decay region along the inhomogeneity direction, is significantly higher than the output power of currently available microwave generators. Analysis of the contradiction between theory [5] and experiment [1–4] has led to significant progress in understanding the nature of observed phenomena and their development scenarios in inhomogeneous plasma [6]. It was shown experimentally [2] and theoretically [6] that low-threshold nonlinear effects typically occur near local plasma density maxima, where two-dimensional localization of daughter waves in the poloidal cross-section is possible, preventing their losses along the plasma inhomogeneity direction from the nonlinear interaction region with the pump wave. Localization occurs due to the excitation of a plasma channel (waveguide) for microwaves along the toroidal direction due to non-monotonic density profile and external magnetic field inhomogeneity [7, 8]. In experiments, non-monotonic density profile behavior is observed both on the discharge axis and in magnetic islands due to transport features in these structures [9]. However, cases where the plasma density profile can be non-monotonic are not limited to these examples. It should be noted that in the edge plasma of current toroidal facilities, there are large-scale coherent structures elongated along magnetic field lines – filaments or blobs – appearing as a result of primary drift wave evolution in the nonlinear stage of low-frequency drift-resistive turbulence development [10]. These structures are related to zonal flows [10] and streamers [11], which are observed in laboratory,

ionospheric, and space plasma. However, unlike zonal flows that lead to drift instability stabilization and thus limit anomalous transport, blobs and filaments, like streamers in dense plasma, are considered responsible for ballistic heat and particle transport across the magnetic field in the rarefied plasma of the wall region in toroidal facilities [12]. As measurements performed by different diagnostic methods show [13, 14], the plasma density in these structures significantly exceeds the background plasma density, with its distribution across the blob being reasonably approximated by a Gaussian function. The latter was also confirmed through gyrokinetic modeling independently performed by various scientific groups [14, 15]. The existence of such structures is associated with the anomalous radiation effect observed at ASDEX-Upgrade tokamak at half-harmonic of the heating microwave radiation in electron cyclotron resonance (ECR) heating experiments [2]. Obviously, similar structures will be present in future reactor-scale facilities. Therefore, the interaction of powerful microwave radiation with these objects represents not only theoretical interest as one of the important nonlinear problems in plasma electrodynamics but also direct practical significance. Until now, close attention has been paid to studying the effects of anomalous microwave radiation and microwave absorption of the extraordinary pump wave, which is typically used in current facilities for ECR plasma heating [2, 16]. At the same time, in the next decade, it is planned to use powerful beams (up to 67 MW) of ordinary microwaves for additional plasma heating and control of neoclassical magnetic islands in the ITER experimental fusion reactor. In particular, to obtain high-density hot plasma, the possibility of using ordinary wave heating at the second ECR harmonic is being discussed [17–19]. Anomalous phenomena in ordinary wave propagation have not been studied in detail until now. In this work, the gap is partially filled by investigating the decay scenario of an ordinary wave with frequency corresponding to the second ECR harmonic, leading to the excitation of two electron Bernstein (EB) waves, two- dimensionally localized in the blob and corresponding to whispering gallery modes [20]. Note that whispering gallery modes are resonant standing waves that can be excited in axisymmetric systems due to total internal reflection. They were first observed for acoustic waves and were investigated by Rayleigh in St. Paul's Cathedral's whispering gallery, from which they got their name [21]. These normal modes are common not only in acoustics problems but also in electrodynamics for gigahertz [22] and terahertz [23] radiation. In particular, their parametric excitation in model experiments was associated with anomalous absorption of microwaves in a linear facility [16].

2. THEORETICAL MODEL

Let us consider the parametric decay instability of an ordinary wave in a blob or filament elongated along the magnetic field line and having a local density maximum in the cross-section. It is quite natural to describe these plasma objects in a local cylindrical coordinate system (r, θ, z), assuming that its origin is located on the filament axis. Following the measurement results and numerical calculations [13–15], we represent the plasma density as the sum of the background density n and the blob density

$$\delta n = \delta n_0 \exp\left(-r^2/r_b^2\right),$$

where δn_0 and r_b are the height and radius of the blob. Since the characteristic scales of background plasma profiles are much larger than the filament radius, which was experimentally confirmed in works [13–15], we will further ignore any spatial dependence except for the inhomogeneity of this structure. We will assume that the temporal variation of the density distribution in the blob is negligibly small, at least during the time of transition of the considered instability into the saturation regime. Let us consider a beam of plane ordinary waves with power P_0, which has a frequency and propagates at ω_0 the edge of plasma across the magnetic field inwards. In the WKB approximation, the pump ordinary wave field in the blob located in the vicinity of the point with coordinate x_b, can be represented as

$$\mathbf{E}_0 = \mathbf{e}_z \frac{E_0(y,z)}{2}\sqrt{\frac{\omega_0}{ck_x(x_b)}} \times$$

$$\times \exp\left(ik_x(x_b)(x - x_b) - i\omega_0 t\right), \qquad (1)$$

where x and z are local Cartesian coordinates along the flux variable and magnetic field respectively, y is the coordinate perpendicular to both of them. In expression (1)

$$k_x = \omega_0\sqrt{\eta(\omega_0)}/c,$$

where

$$\eta = 1 - \omega_{pe}^2/\omega_0^2$$

is the parallel component of the cold plasma dielectric tensor [24], and ω_{pe} is the electron Langmuir frequency. Furthermore, we will assume that the beam width across the magnetic field is much larger than the blob size, $w_{y,z} \gg r_b$. In this case, we can represent (1) in the following form:

$$\mathbf{E}_0 = \mathbf{e}_z \frac{E_0(0,z)}{2}\sqrt{\frac{\omega_0}{ck_x(x_b)}} \times$$
$$\times \sum_{s=-\infty}^{\infty} J_s(k_x(x_b))\exp(is\theta - i\omega_0 t), \quad (2)$$

where J_s is the Bessel function.

Next, we will analyze the decay of an electromagnetic wave into two EB waves with oppositely directed group velocities and frequencies approximately equal to half the pump wave frequency:

$$\omega_{1,2} \simeq \omega_0/2 \leq \omega_{UH},$$

where

$$\omega_{UH} = \sqrt{\omega_{ce}^2 + \omega_{pe}^2}$$

is the upper hybrid frequency, ω_{ce} is the electron cyclotron frequency. The wave numbers of EB waves are solutions of local dispersion equations

$$D_l(\mathbf{q},\omega) = D_{l'}(\mathbf{q},\omega) + iD_{l''}(\mathbf{q},\omega) =$$
$$= q^2 + \chi(\mathbf{q},\omega) + \frac{\omega^2}{c^2}g^2, \quad (3)$$

which take into account resonant and collisional dissipation. The term g^2 in equation (3) describes a small electromagnetic wave component near the upper hybrid resonance (UHR), g is the off-diagonal element of the cold plasma dielectric tensor [24]. The linear plasma susceptibility is given by the known equation [24]

$$\chi = \frac{2\omega_{pe}^2}{\upsilon_{te}^2}\left(1 + \frac{\omega}{|q_z|\upsilon_{te}}\sum_{m=-\infty}^{\infty} Z\left(\frac{\omega - m\omega_{ce}}{q_z\upsilon_{te}}\right)\times\right.$$
$$\left.\times\exp\left(-\frac{q_\perp^2\upsilon_{te}^2}{2\omega_{ce}^2}\right)I_m\left(\frac{q_\perp^2\upsilon_{te}^2}{2\omega_{ce}^2}\right)\right),$$

where Z is the plasma dispersion function, υ_{te} is the electron thermal velocity, I_m is the modified Bessel function. The parametric decay of the pump wave in an axisymmetric blob plasma can lead to the excitation of a pair of whispering gallery EB modes [20], moving in opposite directions along the azimuthal coordinate. The basic set of coupled equations for the daughter wave potentials, describing three-wave interaction at fixed pump wave amplitude, has the form [6]

$$\begin{aligned}\widehat{D}_l\phi_1 + \widehat{D}_{nl}\phi_2 &= 0,\\ \widehat{D}_{nl}\phi_1 + \widehat{D}_l\phi_2 &= 0,\end{aligned} \quad (4)$$

where the integral operators have the form

$$\widehat{D}_{l,nl}f(\mathbf{r},t) =$$
$$= \int \frac{d\omega dt' d\mathbf{q}\, d\mathbf{r}'}{(2\pi)^4} D_{l,nl}\left(\omega,\mathbf{q},\frac{\mathbf{r}+\mathbf{r}'}{2}\right)\times$$
$$\times \exp[i\mathbf{q}\cdot(\mathbf{r}-\mathbf{r}') - i\omega(t-t')]f(\mathbf{r}',t'). \quad (5)$$

In equation (5), the kernel of the linear operator is defined in equation (3), and the kernel of the nonlinear operator equals [25]

$$D_{nl} = \frac{16\omega_{pe}^2\omega_{ce}}{\omega_0(\omega_0^2 - 4\omega_{ce}^2)}\left(iq_z q_r - q_z q_\theta\frac{\omega_{ce}}{\omega_0}\right)\frac{E_0}{\bar{B}}\times$$
$$\times\sqrt{\frac{\omega_0}{ck_x(x_b)}}\sum_{s=-\infty}^{\infty} J_s(k_x(x_b))\exp(is\theta - i\omega_0 t), \quad (6)$$

where $\bar{B}$ is the local value of the external magnetic field. When solving the system of equations (4), we will use the perturbation theory procedure. In the first step, we assume that the damping of daughter waves and nonlinear pumping are weak, and set in equations (4) $D_{l''} = 0$, $D_{nl} = 0$. This reduces the system of coupled equations to two independent linear equations $\hat{D}_l\phi_{1,2} = 0$, the solution of each will be sought in the form

$$\phi_1 = a_1\varphi_p(r)\times$$
$$\times\exp\left(im\theta + iq_z^{p,n}z + i\left(\frac{\omega_0}{2} - \delta\omega^{p,n}\right)t\right),$$
$$\phi_2 = a_2\varphi_n(r)\times$$
$$\times\exp\left(im\theta + iq_z^{p,n}z - i\left(\frac{\omega_0}{2} + \delta\omega^{p,n}\right)t\right), \quad (7)$$

assuming the azimuthal mode number of both waves is large, $m \gg 1$. In this case, the EB wave field will be shifted from the near-axis part of the blob to the UHR region. It localizes near the point r_m, where the condition is met

$$\partial D_{l'}/\partial r|_0 = \partial D_{l'}/\partial r|_{m,q_r} = 0,$$

$$q_\theta = m/r,\quad q_\perp^2 = q_\theta^2 + q_r^2,\quad q_z = 0,\quad \omega_{1,2} = \omega_0/2.$$

The EB wave in this case represents a whispering gallery mode, described by eigenfunctions φ_p and φ_n obeying the reduced differential equation [16]

$$\left(\left|\frac{\partial D_{l'}}{\partial q_\perp}\right|_0 \frac{r_m}{2m}\frac{\partial^2}{\partial r^2} - \left|\frac{\partial^2 D_{l'}}{\partial q_z^2}\right|_0 \frac{(q_z^{p,n})^2}{2} \pm \left|\frac{\partial D_{l'}}{\partial \omega}\right|_0 \delta\omega^{p,n} + \right.$$

$$\left. + D_{l'}|_0 - \left|\frac{\partial^2 D_{l'}}{\partial r^2}\right|_0 \frac{(r-r_m)^2}{2}\right)\varphi_{p,n}(r) = 0. \qquad (8)$$

The eigenvalues $\delta\omega^{p,n}$ and $q_z^{p,n}$ are determined by finding localized solutions of equation (8) and have the form

$$\delta\omega^{p,n} = \pm(p-n)\left|\frac{\partial^2 D_l'}{2\partial r^2}\right|_0^{1/2}\left|\frac{\partial D_l'}{2\partial q_\perp}\right|_0^{1/2}\sqrt{\frac{r_m}{m}}\left|\frac{\partial D_l'}{\partial\omega}\right|_0^{-1},$$

$$q_z^{p,n} = \left|\frac{\partial^2 D_l'}{2\partial q_z^2}\right|_0^{-1/2} \times \qquad (9)$$

$$\times\left(D_l'|_0 - (p+n+1)\left|\frac{\partial^2 D_l'}{2\partial r^2}\right|_0^{1/2}\left|\frac{\partial D_l'}{2\partial q_\perp}\right|_0^{1/2}\sqrt{\frac{r_m}{m}}\right)^{1/2}.$$

In the next step of the perturbation theory procedure, we take into account the damping of daughter waves and their nonlinear excitation, leading to changes in amplitudes $a_{1,2}$ in time and along the magnetic field. Multiplying both sides of equations (4) by complex conjugate zero-order eigenfunctions φ_p and φ_n, which are solutions of equation (8), and performing integration over transverse coordinates, we obtain

$$\left(\frac{\partial}{\partial t} - U_p\frac{\partial}{\partial z} + \nu_{pd}\right)a_1 = i\nu_0(z)a_2,$$

$$\left(\frac{\partial}{\partial t} + U_n\frac{\partial}{\partial z} + \nu_{nd}\right)a_2 = -i\nu_0^*(z)a_1, \qquad (10)$$

where $U_p \simeq U_n = U$ are longitudinal group velocities averaged over the radial localization region of corresponding close radial modes $|p-n|/p \ll 1$ of daughter waves $\nu_{pd} \simeq \nu_{nd} = \nu_d$, and ν_0 are coefficients describing linear damping and inhomogeneous nonlinear pumping. Further, for analytical consideration, we will use a piecewise-defined distribution model of the microwave field along coordinate z:

$$\nu_0(z) = 0, \quad z < -w_z/2,$$

$$\nu_0(z) = \nu_0, \quad -w_z/2 \leqslant z \leqslant w_z/2, \qquad (11)$$

$$\nu_0(z) = 0, \quad w_z/2 < z.$$

The exponentially growing in time solution of the system of equations, $a_{1,2} \propto \exp(\gamma t)$, which behaves continuously at $z = \pm w_z/2$ and exponentially decays at infinity $z \to \pm\infty$, has the following growth-rate

$$\gamma = \nu_0 - U/w_z - \nu_d, \qquad (12)$$

and the threshold is determined by the balance of pumping and losses:

$$\nu_0(P_0^{th}) = U/w_z + \nu_d.$$

3. INSTABILITY THRESHOLD IN VARIOUS EXPERIMENTAL FACILITIES

Let us illustrate the proposed model using the example of two toroidal magnetic plasma confinement facilities. Fig. 1 shows the trajectory of the EB wave (corresponding to azimuthal mode $m = 112$, radial mode $n = 6$ and $f_{m,n} = 70.41$ GHz) [13] for ASDEX-Upgrade tokamak conditions (pump wave frequency $f_0 = 140$ GHz) in the perpendicular cross-section of the blob, obtained using ray-tracing procedure [26], i.e., calculating the trajectory of electromagnetic wave power flow through inhomogeneous magnetized plasma considering its real geometry. The dash-dot line shows the position of the boundary of the blob (r_b =0.6 cm). It can be seen that the wave trajectory envelope is not perfectly circular, which is caused by the influence of the inhomogeneous magnetic field.

In Fig. 2 for the conditions of the Wendelstein 7-X stellarator (pump wave frequency $f_0 = 140$ GHz) [14], the trajectory of the EB wave (corresponding to azimuthal mode $m = 113$, radial mode, $n = 5$, $f_{m,n} = 70.24$ GHz) in the perpendicular cross-section of the blob is shown, also calculated using ray tracing procedure. As in Fig. 1, the dash-dot line shows the position of the blob boundary ($r_b = 0.6$ cm). The EB wave trajectories in Figs. 1 and 2 demonstrate that in both cases these waves do not leave the decay region and correspond to

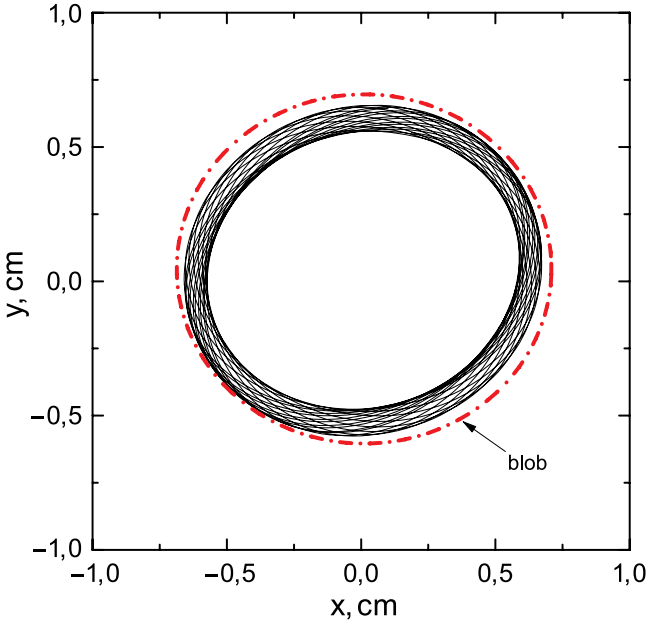

Fig. 1. EB wave trajectory (azimuthal mode $m = 112$, radial mode $n = 6$, $f_{m,n} = 70.41$ GHz) in perpendicular cross-section of the blob for ASDEX-Upgrade tokamak conditions [13]. Dash-dot line – blob boundary position

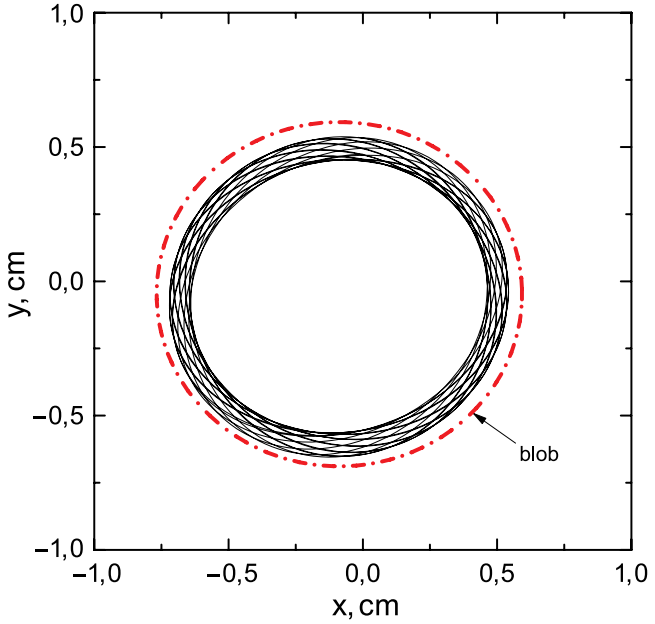

Fig. 2. EB wave trajectory (azimuthal mode $m = 113$, radial mode $n = 5$, and $f_{m,n} = 70.24$ GHz) in perpendicular cross-section of the blob for Wendelstein 7-X stellarator conditions [14]. Dash dot line – blob boundary position

the normal (whispering) mode of the standing wave localized in a narrow region at the blob periphery.

Fig. 3 shows the dependence of the instability growth-rate on the pump power. The theoretical dependencies calculated according to equation (12) for the model rectangular field distribution (11) with size $w_z = 2$ cm are shown by lines. Symbols represent numerical solution results for the Gaussian beam with width $w_y = w_z = 2$ cm. Solid line and circles represent the ASDEX-Upgrade case for experimental parameters specified in work [18]. The threshold value, according to the analytical model (11), (12), equals $P_0^{th} = 297$ kW, and obtained from numerical solving of equations (9) for the Gaussian beam is $P_0^{th} = 282$ kW. Dashed line and diamonds represent the Wendelstein 7-X case for experimental parameters specified in work [19]. The threshold value according to the analytical model equals $P_0^{th} = 285$ kW. The threshold value obtained from calculation is $P_0^{th} = 243$ kW. The difference in threshold values is related to the model representation of the field distribution (11) used in deriving equation (12). At microwave power significantly exceeding the threshold value, the dependencies of the growth-rate on the pump power obtained analytically and numerically asymptotically converge.

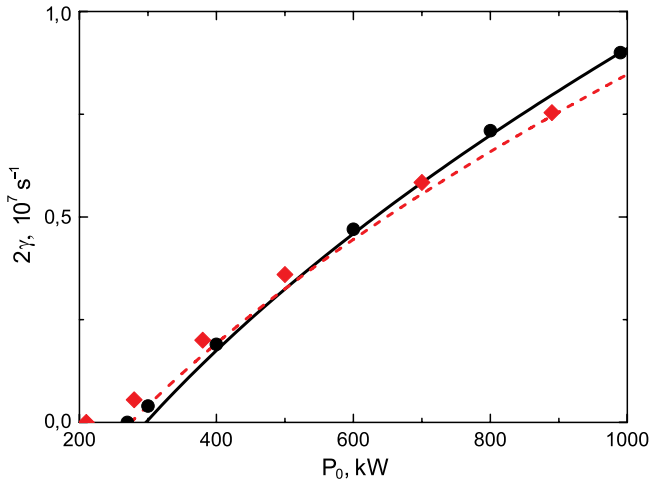

Fig. 3. Dependence of the growth-rate on the pump power. Theoretical dependencies (12) for the model field distribution (11) are shown by lines. The result of numerical solution (of equations (10) for Gaussian beam is shown by symbols. Solid line and circles – the case of ASDEX-Upgrade [18]. Dashed line and diamonds – Wendelstein 7-X [19]. $w_{y,z} = 2$ cm

It should also be noted that the predictions of the developed theory can be verified in a model experiment on the linear facility "Granit" [16], where the plasma column is created by RF discharge in a long glass tube with an internal diameter of $2a = 22$ mm, oriented in the direction of the magnetic field and filled with argon (under pressure

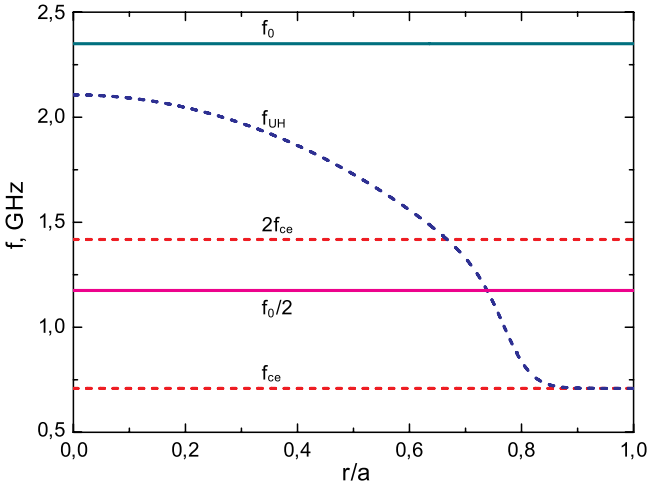

Fig. 4. Frequencies of ECR, second harmonic of ECR, UHR, pump wave and daughter wave in the model experiment

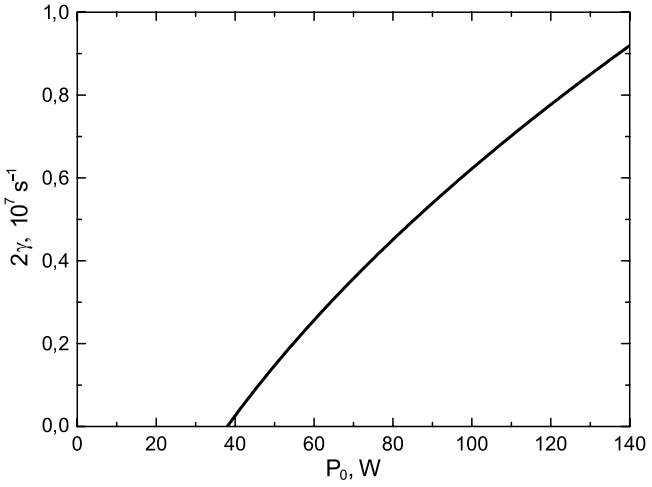

Fig. 6. Dependence of the growth-rate on the pump power in the model experiment. Line – expression (12), $P_0^{th} = 39$ W

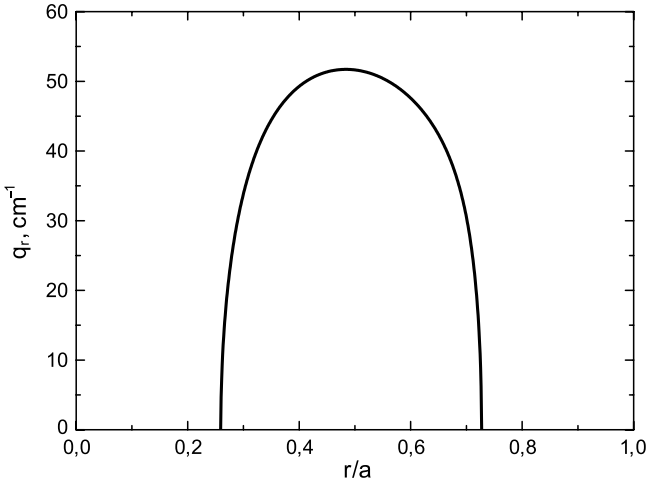

Fig. 5. Radial component of the EB-wave number in the model experiment, $m = 22$, $n_z = 0.9$, $T_e = 1$ eV

of about 10 dyn/cm²). The magnetic field created by an external electromagnet can vary from 0 to 450 G. The volume-averaged plasma density is about 10^{10} см$^{-3}$ and varies by 15–20% with full variation of the magnetic field. The glass tube passes through a hole made in the wide wall of the waveguide (42×34 mm^2) parallel to the narrow wall. Microwave pulses (with power up to 210 W) in the form of ordinary waves are supplied to the plasma along the waveguide. Fig. 4 shows the frequencies of ECR, second harmonic of ECR, UHR, as well as frequencies of the pump wave and daughter wave. Since the frequency of launched waves $f_0 = 2.35$ GHz is higher than the frequency of the second ECR harmonic, $2f_{ce}$, there are no effective linear absorption mechanisms for the pump in the plasma volume, and only the collision mechanism is present, which is weak under experimental conditions. Fig. 5 shows the radial component of the wave number of the daughter EB wave (poloidal mode $m = 22$, longitudinal refractive index $n_z = 0.9$ and $T_e = 1$ eV).

Fig. 6 shows the dependence (12) of the increment of the excited two-plasmon decay instability on power at the electron-atom collision frequency $\nu_{ea} = 5 \cdot 10^6 \text{s}^{-1}$. The estimate for the instability threshold in this case is $P_0^{th} = 39$ W. The predicted instability threshold (about 40 W) is significantly lower than the technically available power of microwave pulses, which allows detailed investigation of this nonlinear phenomenon. In particular, the provided estimates show the possibility to conduct a detailed study of the linear stage of instability and its transition to saturation regime. The latter will allow studying the efficiency of anomalous absorption of the ordinary wave.

4. CONCLUSIONS

For the first time, a scenario of low-threshold decay of an ordinary wave with a frequency corresponding to the second ECR harmonic in the plasma volume has been investigated, leading to the excitation of two EB waves, two-dimensionally localized in a blob (filament) at the plasma edge. Expressions for the growth-rate and threshold of this instability have been obtained. Using equation (12) for the conditions of ASDEX Upgrade and Wendelstein 7-X facilities, threshold values were found. Their values

are significantly lower than the power of megawatt microwave beams used for heating in these facilities. Using the linear facility "Granit" as an example, it is shown that this effect can be studied in model experiments operating with microwave powers up to 200 W. This opens up the possibility for detailed study of this nonlinear phenomenon, including the assessment of the efficiency of anomalous absorption of the ordinary wave.

FUNDING

The results of instability research under model experiment conditions were obtained under Contract No. 23-RB-02-06 and BRFFR project F24SPbG-005. The results of instability research under experimental conditions at ASDEX-Upgrade and Wendelstein 7-X facilities were obtained with support from the Russian Science Foundation (grant No. 22-12-00010), and numerical calculations were performed with support from the state contract of Ioffe Institute of Physics and Technology (FFUG-2024-0028).

REFERENCES

1. *E. Westerhof, S.K. Nielsen, J.W. Oosterbeek et al.*, Plasma Phys. Control. Fusion **55**, 115003 (2013).

2. *S.K. Hansen, S.K. Nielsen, J. Stober et al.*, Nucl. Fusion **60**, 106008 (2020).

3. *A. Tancetti, S.K. Nielsen, J. Rasmussen et al.*, Nucl. Fusion **62**, 074003 (2022).

4. *A. Clod, M.G. Senstius, A.H. Nielsen et al.*, Phys. Rev. Lett. **132**, 135101 (2024).

5. *B.I. Cohen, R.H. Cohen, W. M.C. Nevins, and T.D. Rognlien*, Rev. Mod. Phys. **63**, 949 (1991).

6. *E.Z. Gusakov, A. Yu. Popov*, UFN **190**, 396 (2020).

7. *E.Z. Gusakov and A. Yu. Popov*, Plasma Phys. Control. Fusion **63**, 125017 (2021).

8. *E.Z. Gusakov, A. Yu. Popov*, Plasma Physics **49**, 740 (2023).

9. *M. Yu. Kantor, A. J.H. Donne, R. Jaspers et al.*, Plasma Phys. Control. Fusion **51**, 055002 (2009).

10. *P.H. Diamond, S.-I. Itoh, K. Itoh, and T.S. Hahm*, Plasma Phys. Control. Fusion **47**, R35 (2005).

11. *O.D. Gurcan and P.H. Diamond*, Phys. Plasmas **11**, 572 (2004).

12. *S.I. Krasheninnikov*, Phys. Lett. A **283**, 368 (2001).

13. *B. Nold, G.D. Conway, T. Happel et al.*, Plasma Phys. Control. Fusion **52**, 065005 (2010).

14. *C. Killer, B. Shanahan, O. Grulke et al.*, Plasma Phys. Control. Fusion **62**, 085003 (2020).

15. *J. Cheng, J.Q. Dong, L.W. Yan et al.*, Nucl. Fusion **53**, 093008 (2013).

16. *A.B. Altukhov, V.I. Arkhipenko, A.D. Gurchenko et al.*, Europhys. Lett. **126**, 15002 (2019).

17. *H. Hohnle, J. Stober, A. Herrmann et al.*, Nucl. Fusion **51**, 083013 (2011).

18. *M. Schubert, B. Plaum, S. Vorbrugg et al.*, in *Proc. EPS Conf. on Plasma Physics*, Leuven, Belgium, 4–8 July (2016), Vol. **40A**, P1.026.

19. *T. Klinger, T. Andreeva, S. Bozhenkov et al.*, Nucl. Fusion **59**, 112004 (2019).

20. *K.G. Budden and H.G. Martin*, *The Ionosphere as a Whispering Gallery*, Proc. Roy. Soc. London, Series A. Mathem. Phys. Sci. The Royal Society **265** (1323), 554 (1962).

21. *J.W. Strutt (Lord Rayleigh)*, *Theory of Sound*, Gostekhizdat, Moscow (1955).

22. *P.L. Stanwix, M.E. Tobar, P. Wolf et al.*, Phys. Rev. Lett. **95**, 040404 (2005).

23. *R. Mendis and M. Mittleman*, Appl. Phys. Lett. **97**, 031106 (2010).

24. *D.G. Swanson*, Plasma Waves, 2nd ed., CRC Press (2003).

25. *A. Yu. Popov*, Plasma Physics **48**, 27 (2022).

26. *A. Bernstein, L. Friedland*, in *Fundamentals of Plasma Physics*, Vol. 1. eds. M.N. Rosenbluth and R.Z. Sagdeev, Energoatomizdat, Moscow (1983), p. 393.